ROYAL SOCIETY OF CHEMISTRY

EDGE ARTICLE

Check for updates

Organic photoredox-catalyzed unimolecular PCET of benzylic alcohols†

Tomotoki Matsuo,[a] Masaki Sano,[b] Yuto Sumida 🔟 *[c] and Hirohisa Ohmiya 🔟 *[a]

Proton-coupled electron transfer (PCET) is a crucial chemical process involving the simultaneous or sequential transfer of protons and electrons, playing a vital role in biological processes and energy conversion technologies. This study investigates the use of an organic photoredox catalyst to facilitate a unimolecular PCET process for the generation of alkyl radicals from benzylic alcohols, with a particular focus on alcohols containing electron-rich arene units. By employing a benzophenone derivative as the catalyst, the reaction proceeds efficiently under photoirradiation, achieving significant yields without the need for a Brønsted base. The findings highlight the potential of this unimolecular PCET mechanism to streamline radical generation in organic synthesis, offering a more efficient and flexible alternative to conventional methods.

Proton-coupled electron transfer (PCET) is a fundamental chemical process in which protons and electrons are transferred simultaneously or sequentially (Fig. 1A).[1,2] This process plays a significant role as an elementary step in biological processes (*e.g.*, photosynthesis and cellular respiration) and energy conversion technologies (*e.g.*, fuel cells and solar cells).[3] The PCET reaction combines two basic steps, electron transfer (ET) and proton transfer (PT), which proceed either concertedly or stepwise. The reaction mechanism of PCET is strongly influenced by oxidants and bases. For example, the oxidative PT/ET mechanism predominates when a moderately strong base is used, and an equilibrium concentration of the substrate's conjugate base is present in the reaction solution. The ET/PT-type mechanism also prevails when a moderately strong oxidant is used to oxidise the substrate directly, promoting the activation of more electron-rich substrates. The use of the PCET mechanism for bond cleavage in organic synthesis has not been extensively explored. In the past decade, it has been demonstrated that free alkyl radical intermediates can be generated under mild conditions and directly from readily available starting materials based on the PCET mechanism, with notable contributions by the Knowles group (Fig. 1B-I).[4] They described

that photoredox-catalysed multi-site PCET (MS-PCET) with mild Brønsted bases in a cooperative manner allows the direct generation of energetic intermediates, such as alkoxy radicals from alcohols, despite their high BDFE (*ca.* 105 kcal mol⁻¹).[5] Conventional methods for alkoxy radical generation require the preparation of pre-functionalised radical precursors with readily activatable O–X bonds.[6] These designed precursors can efficiently undergo thermal/photo/radical-induced bond cleavage to generate alkoxy radicals, which serve as synthetically useful intermediates, commonly producing C-centred radicals along with aldehyde or ketone *via* β-scission. Recent advances in alkoxy radical generation have been achieved in conjunction with transition-metal-based photoredox-catalysed, photoinduced PCET and LMCT.[7] More recently, organic photoredox catalysis based on acridinium salt (Fukuzumi catalyst) has served as a strong single-electron oxidant, though examples are limited.[8] Alkyl radicals generated from alcohols have been applied to C–C bond formations, such as Giese addition, Minisci reaction, and Ni-catalysed cross-coupling (Fig. 1B-II).[8] Overall, oxidative MS-PCET enables direct activation of C–H or O/N–H bonds *via* electron and proton transfers to two distinct acceptors. Recent developments typically employ a photoredox catalyst as the electron-transfer agent and a Brønsted base as the proton-transfer reagent separately.[4,6–8] By physically partitioning the photoredox catalyst and proton-transfer reagent, the MS-PCET mechanism covers a broader thermodynamic range and alters chemoselectivity compared to conventional hydrogen atom transfer (HAT) mechanisms, offering more flexibility in reaction conditions. However, this approach is entropically unfavourable and often results in reduced reaction efficiency due to multiple intermolecular interactions. In this context, establishing a unimolecular organic photocatalytic PCET process not only

[a]Institute for Chemical Research, Kyoto University, Gokasho, Uji, Kyoto 611-0011, Japan. E-mail: ohmiya@scl.kyoto-u.ac.jp

[b]Division of Pharmaceutical Sciences, Graduate School of Medical Sciences, Kanazawa University, Kakuma-machi, Kanazawa 920-1192, Japan

[c]Chemical Bioscience Team, Laboratory for Biomaterials and Bioengineering, Institute of Integrated Research, Institute of Science Tokyo, Tokyo 101-0062, Japan. E-mail: sumida.yuto@tmd.ac.jp
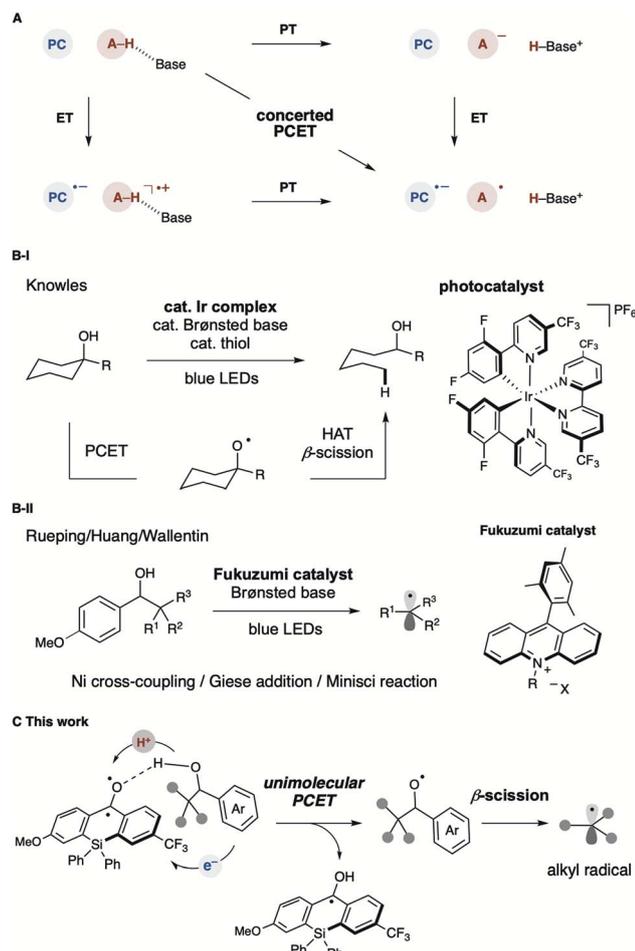
Fig. 1 Proton-coupled electron transfer process (A) schematic model for PCET processes. Flavin-promoted PCET mechanism in biological processes. (B) Ir photoredox-catalysed PCET enabling generation of alkoxy radical. Application of alkyl radical *via* β-scission to organic synthesis. (C) Organic photoredox-catalysed unimolecular PCET enabling alkyl radical generation (this work).

leads to more efficient alkoxy radical generation but also eliminates the previously essential Brønsted base.

We envisioned that the benzophenone catalyst could facilitate the generation of alkyl radicals from alcohols containing electron-rich arene units *via* β-scission through a Brønsted base-free PCET process (Fig. 1C). Benzophenone and its derivatives exhibit closely matched energies in the S1 and T1 states, facilitating almost quantitative and expeditious intersystem crossing ($\varphi_{ISC} = 1.0$, $k_{ISC} = 1 \times 10^{11} \text{ s}^{-1}$).[9] This characteristic enables these molecules to rapidly form excited triplet states upon photoirradiation, leading to oxidation and reduction reactions *via* electron or energy transfer, as well as HAT processes *via* oxygen radicals. In contrast, the unprecedented unimolecular PCET described in this study is achieved by forming a hydrogen bonding network between the carbonyl group of benzophenone and the alcohol, followed by single-electron oxidation in the excited state.

To verify our hypothesis, we initially prepared the benzylic alcohol **1a** as a model substrate having an electron-rich arene

unit, which contributes to efficient reductive quenching of the excited photocatalyst. We evaluated catalytic activity by the production efficiency of aromatic aldehyde **2a** with a variety of benzophenone derivatives. Delightfully, with a catalytic amount of benzophenone (**PC1**) ($E_{red} = +1.53$ V *vs.* SCE in MeCN)[10] and substoichiometric 2,4,6-triisopropylbenzenethiol (TRIP thiol), the reaction of alcohol **1a** provided **2a** in 61% yield under photoirradiation (Table 1, entry 1). Thioxanthone (**PC2**) ($E_{red} = +1.43$ V *vs.* SCE in MeCN)[10] showed higher activity as a photocatalyst, and the product was obtained in high yield even with 1 mol% of the catalyst (entry 2). While anthraquinone (**PC3**), working as a strong oxidant ($E_{red} = +1.98$ V *vs.* SCE in MeCN),[11] afforded the product **2a** in 90% yield, low loading of photocatalyst reduced reaction efficiency (entry 3). We found that silicon-bridged benzophenone derivative **PC4** ($E_{red} = +1.43$ V *vs.* SCE in MeCN)[12] revealed comparable activity with **PC2** and **PC3**

Table 1 Screening of reaction conditions

Entry	Photocatalyst[a]	Yield[b] (%) of 2a
1	Benzophenone (**PC1**)	61
2	Thioxanthone (**PC2**)	83(83)[c]
3	Anthraquinone (**PC3**)	90(65)
4	**PC4**	87(59)[c]
5	**PC5**	77
6	**PC6**	93[d](86)[c]
7	[Ir(dFCF₃ppy)₂(dtbpy)]PF₆ (**PC7**)	0[c]
8	[(*t*Bu)₂MesAcr]BF₄ (**PC8**)	6[c]
9	4CzIPN (**PC9**)	17[c]
10	C₆H₅SH instead of TRIP thiol	84[e]
11	*n*-Dodecanethiol instead of TRIP thiol	28
12	W/o thiol	12[e]
13	MeCN instead of CH₂Cl₂	80[e]
14	W/o photocatalyst	0
15	Under dark	0[e]
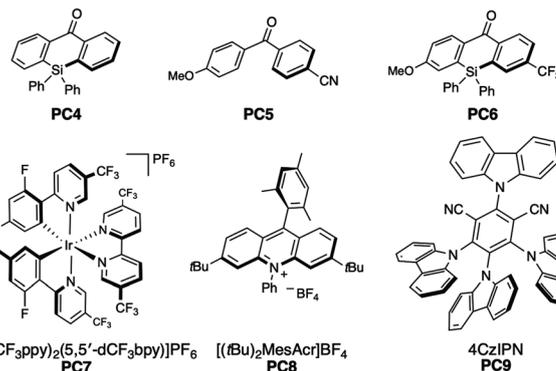
[a] Reaction was carried out with **1a** (0.1 mmol), photocatalyst (5 μmol), and TRIP thiol (0.05 mmol) in CH₂Cl₂ (1 mL) under 390 nm blue LED (Kessil lamp) irradiation at ambient temperature for 2 h. [b] ¹H NMR yield. [c] 1 mol% of photocatalyst was used. [d] Isolated yield. [e] 5 mol% of **PC6** was used as photocatalyst.

(entry 4). Consequently, we evaluated disubstituted benzophenone catalyst **PC5**, bearing an electron-withdrawing and an electron-donating group on each arene, reported by the Molander group ($E_{red}^* = +1.75$ V vs. SCE in MeCN),[13] and higher yield was observed compared to unsubstituted benzophenone **PC1** (entry 5). This result can be attributed to the captodative effect, which stabilises both the triplet ketyl radical and the protonated radical intermediate via PCET. Consequently, we designed and synthesised the push–pull type silicon-bridged benzophenone **PC6**, which exhibited the most effective catalytic activity for PCET-promoted β-scission (entry 6). Several conventional photoredox catalysts used in recent PCET chemistry were also evaluated without Brønsted bases. In the presence of [Ir(dFCF₃ppy)₂(5,5′-dCF₃bpy)]PF₆ (**PC7**) ($E_{red} = +1.68$ V vs. SCE in MeCN),[14] no reaction of **1a** was observed. Despite the advantage of its high reduction potential in the excited state, only a low yield of aldehyde **2a** was obtained when using [(tBu)₂MesAcr]BF₄ (**PC8**) ($E_{red} = +2.15$ V vs. SCE in MeCN),[15] a photocatalyst effective for PCET in the presence of Brønsted base (entry 8). The reaction using 4CzIPN (**PC9**) ($E_{red}^* = +1.43$ V vs. SCE in MeCN),[16] which has a redox potential comparable to **PC6**, provided product **2a** in a 17% yield (entry 9). We also investigated the effects of thiols and solvents. Arylthiol had no significant influence on yield (entry 10), whereas aliphatic thiol or the absence of thiol as an additive significantly hindered product formation (entries 11 and 12). Solvent changes had little impact on the reaction outcome (entry 13, see ESI†). It was confirmed that no reaction occurred without photocatalyst or photoirradiation (entries 14 and 15). Considering the mechanism of photoredox reactions, the redox potentials of photocatalysts and substrates are critical factors for catalytic activity. Therefore, we calculated the redox potentials for the reductive quenching of benzophenone derivatives and other photocatalysts, including **PC7**–**PC9**, to optimise reaction conditions (Table 1). However, no clear correlation with yields was observed (Fig. 2A). Absorption wavelength, molar absorption coefficient, and excitation lifetime also affect photoredox catalysis efficiency. Among the photocatalysts that gave high yields, the push–pull type benzophenone catalysts **PC5** and **PC6** displayed red-shifted absorptions compared to the unsubstituted benzophenones **PC1** and **PC4**. Thioxanthone (**PC2**) and anthraquinone (**PC3**), which also showed high catalytic activity, had relatively longer absorption wavelengths, extending to around the reaction wavelength of 390 nm, although their molar absorption coefficients were low (Fig. 2B). These results suggest that wavelength may influence catalytic efficiency. Subsequently, we evaluated the triplet state and redox potential of **PC6** using computational calculations, UV/vis spectroscopy, fluorescence, and cyclic voltammetry (Fig. 2B and D). The Kohn–Sham orbital, calculated at the UM062X/6-311++G(d,p) level, showed the distribution of the LUMO (Fig. 2C). The excited state of benzophenone acts as a biradical, with the C–O bond lengthening from 1.22 Å to 1.33 Å compared to the C=O bond in the X-ray structure[17] (Fig. 2E).

The **PC6**-catalysed β-scission of electron-rich benzylic alcohols via unimolecular photo-PCET demonstrated excellent functional group compatibility (Fig. 3A). Reactions were
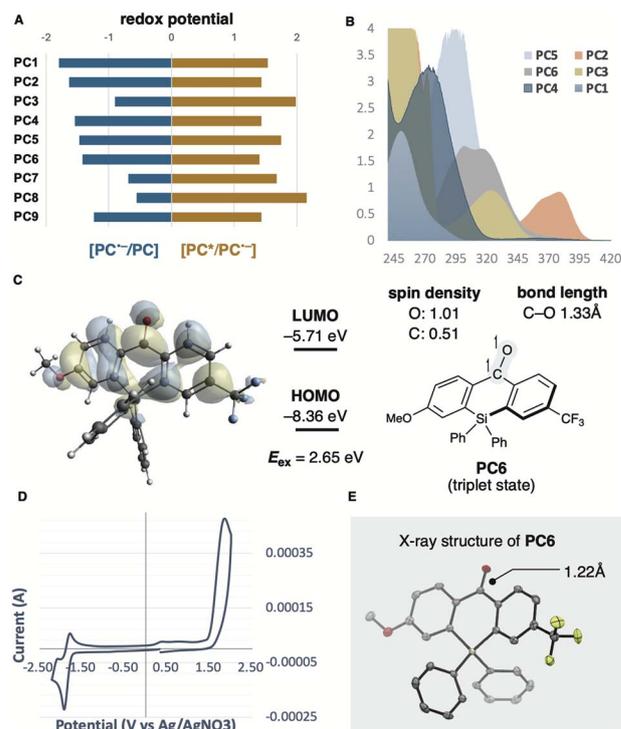

Fig. 2 (A) Redox potentials for reductive quenching of **PC1–9**. (B) UV/vis spectra of **PC1–PC6** (20 μM in MeCN). (C) Triplet state energies and structural property of **PC6** calculated by DFT at the UM062X/6-311++G(dp) level. (D) Cyclic voltammogram **PC6** (100 μM in MeCN), electrolyte: nBu₄NClO₄ RE: Ag/AgNO₃, WE: glassy carbon, CE: Pt wire. (E) ORTEP diagram of **PC6** (CCDC 2352222).

conducted under optimised conditions: using dichloromethane as solvent, exposure to blue LED light at 390 nm for two hours, 5 mol% **PC6** as catalyst, and a substoichiometric amount of TRIP thiol as a co-catalyst. The effects of each additive (**A1–A26**) were assessed in terms of aldehyde **2a** formation and additive recovery.[18] Fortunately, almost all additives had no significant effect on the target transformation, with quantitative recovery of additives. Despite the HAT ability of benzophenone-type catalysts, additives containing benzylic protons did not inhibit the β-scission process, and aldehyde **2a** was obtained in high yield with quantitative recovery of **A1** or **A2**. Additives **A3–9**, containing reactive functional groups or protic compounds, such as alcohols and acids (**A10–12**), were also ineffective.

Recent reports of catalytic photo-PCET of alcohols or amides usually require a base for concerted deprotonation, suggesting that acidic substrates may not be compatible. However, some additives showed moderate to low efficiency in the PCET process, affecting either conversion rates or additive recovery.

For instance, additive **A13** (thiol) resulted in a 68% conversion rate and 77% recovery of thiol, while **A14** (benzylamine) had a detrimental effect, with a 51% conversion and no recovery. Additives **A18**, **A24**, and **A25** affected alcohol **1a** conversion, while **A23** and **A26** resulted in low additive recovery, likely due to undesired alkyl radical addition pathways. Although **A25** could act as a hydrogen atom transfer (HAT) donor or a mild base, comparison with the calculated BDFEs for
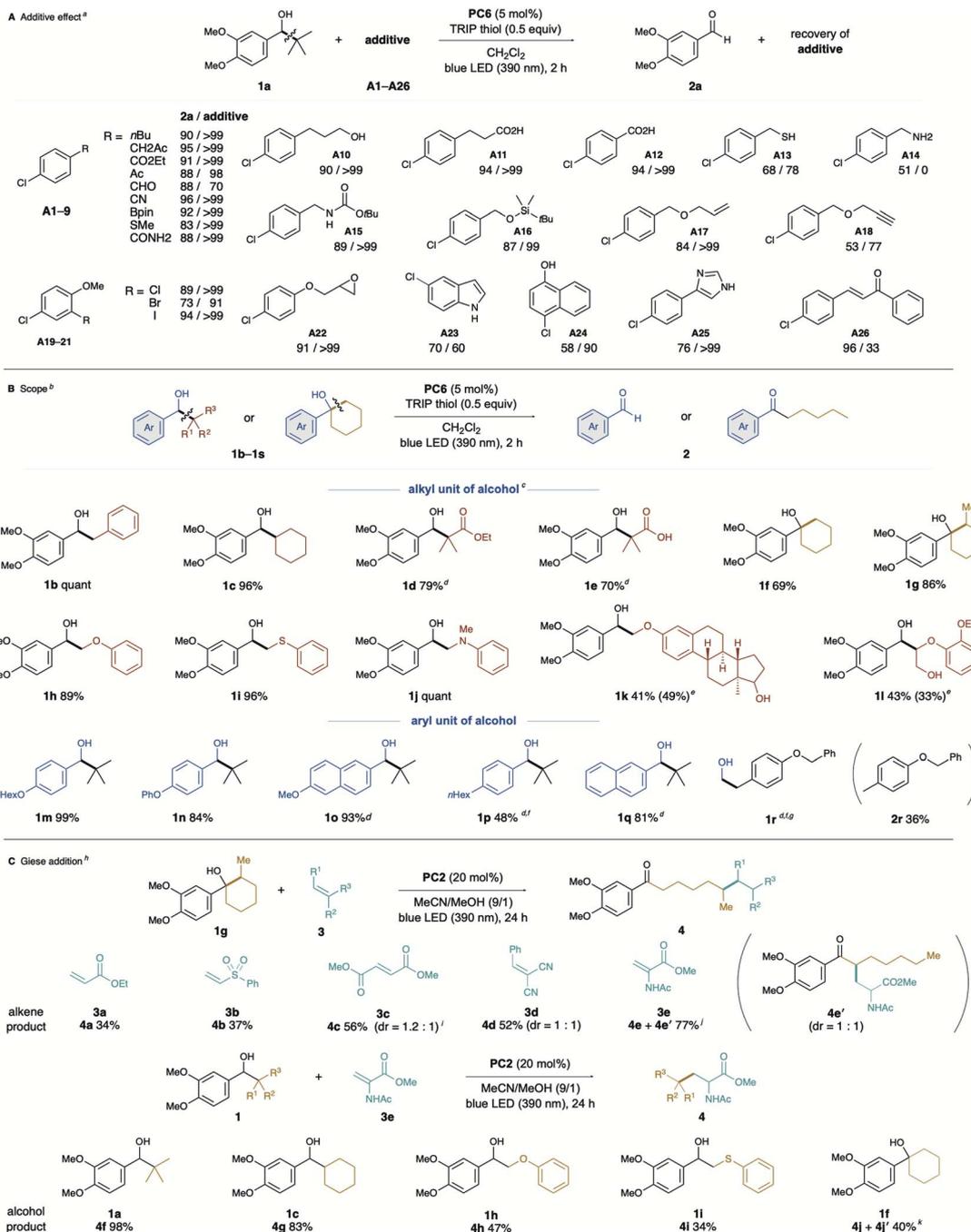
Fig. 3 (A) Additive effect on catalytic photo-PCET. (a) 1 equivalent of additive was added. (B) Substrate scope of alcohols. (b) *Cis*-isomerisation was observed. (c) Reaction was carried out with **1** (0.2 mmol), **PC6** (0.01 mmol), and TRIP thiol (0.1 mmol) in CH$_2$Cl$_2$ (2 mL) under 390 nm blue LED (Kessil lamp) irradiation at ambient temperature for 2 h. (d) Anthraquinone was used as a photocatalyst. (e) Yield of HAT product in parenthesis. (f) 10 mol% of photocatalyst was used. (g) Reaction was stirred for 6 h. (C) Giese addition (h) reaction was carried out with **1** (0.3 mmol), **PC2** (0.04 mmol), and alkene **3** (0.2 mmol) in MeCN/MeOH (9/1, 2 mL) under 390 nm blue LED (Kessil lamp) irradiation at ambient temperature for 24 h. (i) Reaction was carried out with **1g** (0.2 mmol), **PC2** (0.04 mmol), and alkene **3** (0.4 mmol) in MeCN (2 mL) under 390 nm blue LED (Kessil lamp) irradiation at ambient temperature for 24 h. (j) **4e** : **4e′** = 1.8 : 1, dr of **4e** = 1 : 1. (k) **4j** : **4j′** = 1 : 1.9, dr of **4j′** = 1 : 1.3.

thiol (81.6 and 67.5 kcal mol^{-1}) suggests no significant impact on the reaction (see ESI†).

Next, we investigated the substrate scope (Fig. 3B), using **PC6** as an organic photocatalyst to initiate unimolecular PCET, leading to the formation of aldehydes or ketones *via* β-scission of the hydroxyl group. The substrate scope included various

alcohols with different substituents, demonstrating the versatility of the reaction. Initially, we examined alkyl units generating the alkyl radical from substrates with electron-rich arenes. In addition to **1a**, which has *t*Bu groups, substrates with benzyl and cyclohexyl groups (**1b** and **1d**) gave 3,4-dimethoxybenzaldehyde (**2a**) efficiently. β-Hydroxyesters **1d** and **1e**, easily

prepared by the Aldol reaction, also yielded **2a** in high yields. This suggests that the C–C bond formed in the two-electron process can behave as an alkyl radical *via* β-scission. Additionally, **1e**, with an intramolecular carboxylic acid, was challenging for conventional photocatalyst-base cooperative PCET but performed well here. Ring-opening occurred in the case of cyclic alkyl alcohols, such as **1f** and **1g**, yielding the corresponding ketones **2f** and **2g**. Similarly, alcohols with a heteroatom substituted at the β-position, such as **1h**, **1i**, and **1j**, were easily synthesised by nucleophilic substitution of the corresponding α-bromoketone with a nucleophile such as alcohol, followed by reduction of the carbonyl group. C–C bond cleavage proceeded efficiently with these substrates, and **2a** was obtained in high yield. In the estradiol derivative **1k**,[8d] while PCET proceeded only with the electron-rich arene-substituted alcohol, the other alcohol unit remained intact, yielding aldehyde **2a** and a product in which the phenolic hydroxyl group of estradiol was formally methylated. Furthermore, photo-PCET has recently gained attention as a powerful tool in lignin degradation,[19] a representative biomass. Our catalytic photo-PCET system similarly worked with the lignin model molecule **1l**, leading to degradation that afforded the corresponding aldehydes **2a** and phenols. Next, we examined the reaction efficiency by varying the aryl unit of the substrate.

The monoalkoxy-substituted substrate **1m** achieved quantitative conversion, showcasing the reaction's applicability with different structural motifs. The phenoxy group-substituted substrate **1n** yielded the corresponding aldehyde in 84%, further illustrating the effectiveness of the method. Using anthraquinone (**PC3**) as a photocatalyst, which acts as a stronger oxidant, alcohols with less activated arenes, such as naphthyl and alkylphenyl-substituted alcohols (**1o**, **1p**, and **1q**), were successfully converted into the corresponding aldehydes. Pleasingly, non-benzylic alcohol **1r** was also applicable to our catalytic system, yielding **2r** in moderate yield *via* C–C bond cleavage, with formaldehyde also formed. We then explored the potential of this method for generating alkyl radicals from aliphatic alcohols (Fig. 3C). After re-screening the photocatalytic conditions for Giese addition, we found that **PC2**, thioxanthone, provided the best results. We attribute this to the distinct mechanism of the Giese addition, which slightly alters the required photocatalytic performance. The β-alkylation of acrylate **3a** and vinylsulfone **3b** proceeded, albeit with low yields of the corresponding products **4a** and **4b**. The reaction of malonate **3c** and benzylidene malononitrile **3d**, both more electron-deficient alkenes, afforded moderate yields (**4c** and **4d**). Fortunately, high efficiency in alkyl radical addition was observed with dehydroalanine derivative **3e**, suggesting that this protocol could be applied to protein modification.[20] Whereas the reaction using **1g** as an alkyl radical source resulted in a regioisomeric mixture (**4e** + **4e′**), the regioisomer **4e′** likely formed *via* a 1,5-HAT process after PCET-promoted ring-opening β-scission of **3e**. Based on the bond dissociation energy (BDE) comparison between a typical C–H bond (100 kcal mol^{-1})[21] and an α-carbonyl C–H bond (92 kcal mol^{-1}),[22] intramolecular HAT can readily occur, thus allowing the generated α-carbonyl radical to attack **3e**, forming the regioisomer **4e′**. We also explored the

alcohol scope in Giese addition. Using alcohols **1a** and **1c**, which generate tertiary-butyl and cyclohexyl radicals, Giese addition produced high yields of the corresponding adducts (**4f** and **4g**). This method also enabled the generation of α-oxy and α-thiomethyl radicals, applying them to radical additions that furnished the corresponding products **4h** and **4i**. The electron-rich arene-pendant cyclohexanol **1f** gave results similar to **1g**, producing a regioisomer **4j′** *via* the intramolecular HAT process.

To gain insight into the reaction mechanism, we conducted several experiments and photophysical analyses. Minisci-type reaction was investigated using lepidine treated with trifluoroacetic acid as a substrate (Fig. 4A). When MnO$_2$ was used as an oxidant in the presence of **PC6**, the corresponding alkylated product **5** was obtained in good yield, suggesting that our protocol can work even under acidic conditions and expanding its versatility. Using a stoichiometric amount of thioxanthone (**PC2**) in the presence of the radical trapping reagent TEMPO, the reaction afforded the *t*Bu radical adduct **7** in 55% yield. This suggests the formation of alkoxy radicals, followed by β-C–C bond cleavage to generate alkyl radicals (Fig. 4B). We also examined the interaction between the photocatalyst and the substrate in the reaction solution and the formation of charge transfer complexes (EDA complexes). The UV-vis spectrum of each component was measured, as well as that of the mixture (Fig. 4C). As a result, no data supporting the formation of an EDA complex were obtained. Substrate **1a** exhibited no absorption in the visible light range as expected (Fig. 4C, red line), and no change in the absorption spectrum was observed for the mixture of **PC2** and **1a**. A photo-quenching experiment (Stern–Volmer plot) also provided mechanistic insight into the organic catalytic photo-PCET process. While no photo-quenching was observed for thioxanthone (**PC2**) with TRIP thiol (Fig. 4D, blue line), the Stern–Volmer plot for the substrate in the presence of **PC2** showed significant photo-quenching of the photocatalyst (Fig. 4D, yellow line). Given the redox potential of **PC6** [E_{red}(PC*/PC$^{•-}$) = +1.43 V *vs.* SCE] and 1,2-dimethoxybenzene [E_{ox} = 1.42 V *vs.* SCE],[23] SET oxidation of the substrate was feasible, but the SET efficiency for other benzylic alcohols with higher oxidation potentials, such as **1m–1s**, could be significantly lower.

To further understand the reaction mechanism, we used computational methods to evaluate plausible pathways and energy profiles (Fig. 4E). The triplet state (T1) of the silicon-bridged benzophenone exhibited a higher energy level. Interestingly, the triplet state (T1) formed a highly stabilised complex through interaction with substrate **1a**, which we defined as the starting point (0 kcal mol^{-1}). The pathways leading to the formation of alkoxy and ketyl radicals (**INT1**) *via* transition state **TS1** are proposed to involve either concerted electron/proton transfer (CEPT) or a stepwise electron transfer followed by proton transfer (ET/PT). However, distinguishing between these two pathways using DFT calculations proved challenging. **TS2** represents the transition state for the formation of the *t*Bu radical *via* C–C bond cleavage of the generated alkoxy radical. Although the energy of **TS2** was relatively high at 17.9 kcal mol^{-1}, this value was reasonable. Based on experimental, analytical, and computational analyses, we propose the
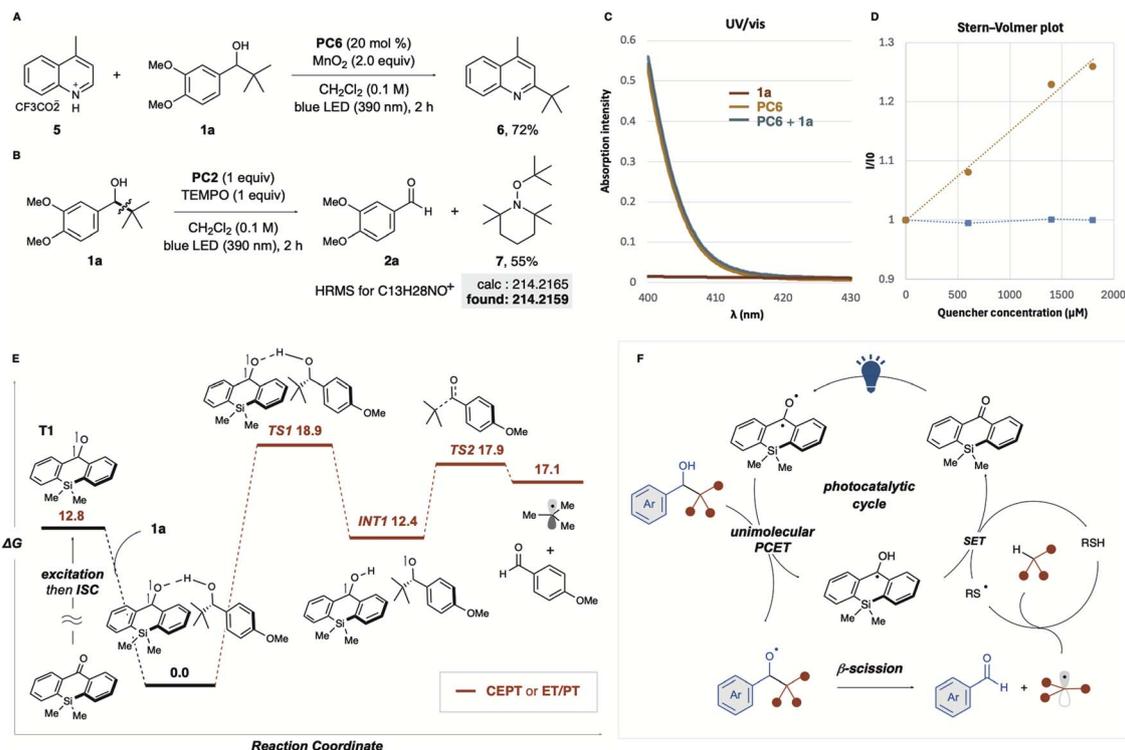
Fig. 4 (A) Minisci-type reaction (B) radical trapping experiment (C) UV-vis absorption spectra of substrates. (D) Photo-quenching experiment. Yellow line (●): **PC2** (200 μM) with alcohol **1a**. Blue line (■): photocatalyst (40 μM) with TRIP thiol. (E) Energy profiles for the proposed pathway. Density functional theory calculations were carried out at the (U)M06-2X/6-311+G(d,p) level of theory, the unit of Gibbs free energies (ΔG) is kcal mol^{-1}. (F) Plausible mechanism.

catalytic mechanism outlined in Fig. 4F. Unimolecular PCET of the excited photocatalyst with electron-rich benzyl alcohol derivatives generates an alkoxy radical, followed by β-C–C bond cleavage to form alkyl radicals and aldehydes. HAT with the cocatalytic thiol quenches the resulting alkyl radicals, forming thiyl radicals. Finally, ET/PT occurs between the ketyl radical and the thiyl radical, regenerating the catalyst. BDFE analysis provides additional support for the proposed PCET mechanism. The O–H bond dissociation free energy (BDFE) of the optimal catalyst **PC6** (95.8 kcal mol^{-1}) closely matches that of the substrate alcohol (95.5 kcal mol^{-1}), enabling efficient hydrogen atom transfer. In contrast, thioxanthone, which has a higher BDFE (98.9 kcal mol^{-1}), demonstrates slightly reduced activity, likely due to its less favourable energy match with the substrate. Furthermore, the thiol cocatalyst's low BDFE (67.5 kcal mol^{-1}) highlights its role as HAT donor, facilitating the regeneration of the photocatalyst during the catalytic cycle. Considering that the Giese addition proceeds efficiently without the addition of thiol, thiol is not strictly required for the generation of alkyl radicals *via* the PCET process. Nonetheless, in the HAT system with thiol addition, it remains possible that the thiolate, generated through the reduction of the thiyl radical, acts as a mild base to facilitate the PCET process.

facilitates the generation of alkyl radicals from alcohols containing electron-rich arene units. The base-free PCET enables β-scission of substrates with protic functional groups, including carboxylic acids, probably due to the formation of a hydrogen-bonding network between the excited triplet state of benzophenone and the hydroxy group. This method presents a more efficient and flexible alternative to conventional approaches, with potential applications in C–C bond formations and other organic transformations.

Data availability

The data supporting this article have been included as part of the ESI.†

Author contributions

T. M., M. S., Y. S., and H. O. designed, performed and analysed the experiments. Y. S. and H. O. co-wrote the manuscript. All authors contributed to discussions.

Conclusions

In summary, we developed a Brønsted base-free, unimolecular PCET process catalysed by a benzophenone-type catalyst, which

Conflicts of interest

There are no conflicts to declare.

Acknowledgements

Notes and references

1 (a) D. R. Weinberg, C. J. Gagliardi, J. F. Hull, C. F. Murphy, C. A. Kent, B. C. Westlake, A. Paul, D. H. Ess, D. G. McCafferty and T. J. Meyer, *Chem. Rev.*, 2012, **112**, 4016–4093; (b) J. W. Darcy, B. Koronkiewicz, G. A. Parada and J. M. Mayer, *Acc. Chem. Res.*, 2018, **51**, 2391–2399; (c) J. M. Mayer and I. J. Rhile, *Biochim. Biophys. Acta, Bioenerg.*, 2004, **1655**, 51–58.

2 P. R. D. Murray, J. H. Cox, N. D. Chiappini, C. B. Roos, E. A. McLoughlin, B. G. Hejna, S. T. Nguyen, H. H. Ripberger, J. M. Ganley, E. Tsui, *et al.*, *Chem. Rev.*, 2022, **122**, 2017–2291.

3 (a) K. Mittra and M. T. Green, *J. Am. Chem. Soc.*, 2019, **141**, 5504–5510; (b) T. H. Yosca, J. Rittle, C. M. Krest, E. L. Onderko, A. Silakov, J. C. Calixto, R. K. Behan and M. T. Green, *Science*, 2013, **342**, 825–829; (c) L. A. Büldt and O. S. Wenger, *Chem. Sci.*, 2017, **8**, 7359–7367; (d) K. Kalyanasundaram, *Coord. Chem. Rev.*, 1982, **46**, 159–244.

4 (a) H. G. Yayla, H. Wang, K. T. Tarantino, H. S. Orbe and R. R. Knowles, *J. Am. Chem. Soc.*, 2016, **138**, 10794–10797; (b) E. Ota, H. Wang, N. L. Frye and R. R. Knowles, *J. Am. Chem. Soc.*, 2019, **141**, 1457–1462; (c) K. Zhao, K. Yamashita, J. E. Carpenter, T. C. Sherwood, W. R. Ewing, P. T. W. Cheng and R. R. Knowles, *J. Am. Chem. Soc.*, 2019, **141**, 8752–8757; (d) E. Tsui, A. J. Metrano, Y. Tsuchiya and R. R. Knowles, *Angew. Chem., Int. Ed.*, 2020, **59**, 11845–11849.

5 S. J. Blanksby and G. B. Ellison, *Acc. Chem. Res.*, 2003, **36**, 255–263.

6 (a) L. Chang, Q. An, L. Duan, K. Feng and Z. Zuo, *Chem. Rev.*, 2022, **122**, 2429–2486; (b) E. Tsui, H. Wang and R. R. Knowles, *Chem. Sci.*, 2020, **11**, 11124–11141; (c) S. P. Morcillo, *Angew. Chem., Int. Ed.*, 2019, **58**, 14044–14054; (d) K. Jia and Y. Chen, *Chem. Commun.*, 2018, **54**, 6105–6112; (e) D. S. Finis and D. A. Nicewicz, *J. Am. Chem. Soc.*, 2024, **146**, 16830–16837; (f) K. Jia, F. Zhang, H. Huang and Y. Chen, *J. Am. Chem. Soc.*, 2016, **138**, 1514–1517.

7 (a) J.-J. Guo, A. Hu, Y. Chen, J. Sun, H. Tang and Z. Zuo, *Angew. Chem., Int. Ed.*, 2016, **55**, 1531–15322; (b) A. Hu, Y. Chen, J.-J. Guo, N. Yu, Q. An and Z. Zuo, *J. Am. Chem. Soc.*, 2018, **140**, 13580–13585; (c) A. Hu, J.-J. Guo, H. Pan, H. Tang, Z. Gao and Z. Zuo, *J. Am. Chem. Soc.*, 2018, **140**, 1612–1616; (d) A. Hu, J.-J. Guo, H. Pan and Z. Zuo, *Science*, 2018, **361**, 668–672; (e) Y. Chen, X. Wang, X. He, Q. An and Z. Zuo, *J. Am. Chem. Soc.*, 2021, **143**, 4896–4902; (f) W. Liu, Q. Wu, M. Wang, Y. Huang and P. Hu, *Org. Lett.*, 2021, **23**,

8413–8418; (g) L. Wen, J. Ding, L. Duan, S. Wang, Q. An, H. Wang and Z. Zuo, *Science*, 2023, **382**, 458–464.

8 (a) L. Huang, T. Ji and M. Rueping, *J. Am. Chem. Soc.*, 2020, **142**, 3532–3539; (b) K. Liao, F. Wu, J. Chen and Y. Huang, *Cell Rep. Phys. Sci.*, 2022, **3**, 100763; (c) N. Salaverri, B. Carli, P. B. Gratal, L. Marzo and J. Alemán, *Adv. Synth. Catal.*, 2022, **364**, 1689–1694; (d) Y. Patehebieke, R. Charaf, H. P. Bryce-Rogers, K. Ye, M. Ahlquist, L. Hammarström and C.-J. Wallentin, *ACS Catal.*, 2024, **14**, 585–593.

9 N. A. Romero and D. A. Nicewicz, *Chem. Rev.*, 2016, **116**, 10075–10166.

10 (a) H. J. Timpe and K. P. Kronfeld, *J. Photochem. Photobiol., A*, 1989, **46**, 253–267; (b) H. J. Timpe, K. P. Kronfeld, U. Lammel, J. P. Fouassier and D. J. Lougnot, *J. Photochem. Photobiol., A*, 1990, **52**, 111–122.

11 J. E. Bachman, L. A. Curtiss and R. S. Assary, *J. Phys. Chem. A*, 2014, **118**, 8852–8860.

12 See ESI.†

13 M. W. Campbell, M. Yuan, V. C. Polites, O. Gutierrez and G. A. Molander, *J. Am. Chem. Soc.*, 2021, **143**, 3901–3910.

14 Q. Zhu, E. C. Gentry and R. R. Knowles, *Angew. Chem., Int. Ed.*, 2016, **55**, 9969–9973.

15 N. A. Romero, K. A. Margrey, N. E. Tay and D. A. Nicewicz, *Science*, 2015, **349**, 1326–1330.

16 (a) H. Uoyama, K. Goushi, K. Shizu, H. Nomura and C. Adachi, *Nature*, 2012, **492**, 234–238; (b) E. Speckmeier, T. G. Fischer and K. Zeitler, *J. Am. Chem. Soc.*, 2018, **140**, 15353–15365.

17 Y. Sumida, *CSD Communication*, 2024, DOI: 10.5517/ccdc.csd.cc2jyp4b.

18 N. Saito, A. Nawachi, Y. Kondo, J. Choi, H. Morimoto and T. Ohshima, *Bull. Chem. Soc. Jpn.*, 2023, **96**, 465–474.

19 (a) J. D. Nguyen, B. S. Matsuura and C. R. J. Stephenson, *J. Am. Chem. Soc.*, 2014, **136**, 1218–1221; (b) I. Bosque, G. Magallanes, M. Rigoulet, M. D. Kärkäs and C. R. J. Stephenson, *ACS Cent. Sci.*, 2017, **3**, 621–628; (c) W. Zhou, J. Nakahashi, T. Miura and M. Murakami, *Asian J. Org. Chem.*, 2018, **7**, 2431–2434; (d) G. Magallanes, M. D. Kärkäs, I. Bosque, S. Lee, S. Maldonado and C. R. J. Stephenson, *ACS Catal.*, 2019, **9**, 2252–2260; (e) S. T. Nguyen, P. R. D. Murray and R. R. Knowles, *ACS Catal.*, 2020, **10**, 800–805; (f) Y. Wang, J. He and Y. Zhang, *CCS Chem.*, 2020, **2**, 107–117; (g) Y. Li, J. Wen, S. Wu, S. Luo, C. Ma, S. Li, Z. Chen, S. Liu and B. Tian, *Org. Lett.*, 2024, **26**, 1218–1223.

20 B. Josephson, C. Fehl, P. G. Isenegger, S. Nadal, T. H. Wright, A. W. J. Poh, B. J. Bower, A. M. Giltrap, L. Chen, C. Batchelor-McAuley, *et al.*, *Nature*, 2020, **585**, 530–537.

21 L. Capaldo, D. Ravelli and M. Fagnoni, *Chem. Rev.*, 2022, **122**, 1875–1924.

22 P. C. St. John, Y. Guan, Y. Kim, S. Kim and R. S. Paton, *Nat. Commun.*, 2020, **11**, 2328.

23 P. Luo, E. C. Feinberg, G. Guirado, S. Farid and J. P. Dinnocenzo, *J. Org. Chem.*, 2014, **79**, 9297–9304.